Journal of Engineering and Sustainable Development
https://jeasd.uomustansiriyah.edu.iq/index.php/jeasd
https://doi.org/10.31272/jeasd.27.6.10

Vol. 27, No. 06, November 2023
ISSN 2520-0917

Original Research

RECONFIGURABLE GRAPHENE-BASED MULTI-INPUT-MULTI-OUTPUT ANTENNA FOR SIXTH GENERATION AND BIOMEDICAL APPLICATIONS

Reem Hikmat Abd[*1], Hussein A. Abdulnabi[2]

Electrical Engineering Department, College of Engineering, Mustansiriyah University, Baghdad, Iraq
[1]https://orcid.org/0000-0002-2438-7225
[2]https://orcid.org/0000-0002-2156-2710

Received 04/01/2023 ***Revised 20/03/2023*** ***Accepted 27/04/2023***

Abstract: In this paper, a small MIMO antenna with a semi-hexagonal form is developed for use in terahertz applications. The suggested antenna consists of four radiating components printed on a Silicon Dioxide substrate that is 90 ×90 μm^2, with a thickness of 10 µm. The radiating components have been positioned in an orthogonal orientation to produce excellent isolation and miniaturization of the MIMO system. The suggested MIMO antenna works for all the (0.1-10)THz bands with different values of chemical potential with wide impedance bandwidth (S11 ≤ -10dB) in the frequency range of 2.4 to more than 10 THz, With a co-reflection coefficient less than -20 dB over the whole operating band, with a return loss -50 dB. The MIMO antenna has a maximum gain of 8.4 dBi and a steady diversity performance across all the working bands. According to the high-performance characteristics, the suggested graphene MIMO antenna design can be used for many applications in the THz band, including 6G high-speed wireless communication systems, security scanning, biomedical applications, IoT (Internet of Things), and sensing.

Keywords: *Chemical potential; graphene; isolation; semi-hexagonal; Terahertz applications*

1. Introduction

Recent years have seen an increased demand for the unused frequency spectrum. For higher carrier frequency, future communication systems focus on the THz area, more channel capacity, and better data speeds [1]. On the electromagnetic spectrum, terahertz radiation is emitted between infrared and microwave radiation in the range of 0.1–10 THz. hence has numerous features with these other forms of radiation. Similar to infrared and microwave radiation, terahertz radiation is non-ionizing and travels straight through materials. Identical to microwave radiation, Terahertz radiation may pass through various non-electrically conducting materials [2].

Between (2027 and 2030) years anticipated that the sixth-generation (6G) wireless communication system, a new wireless communication paradigm, will be deployed. This system will have the full support of artificial intelligence. The infrastructure for sixth-generation (6G) wireless communications will demand frequency working at terahertz frequencies [3,4]. Due to a lack of available equipment, materials, measurements [5], detectors, and sources that work within the terahertz band, the band of the electromagnetic spectrum that was concerned with the development of the 6 G with terahertz frequency was the one that got the most amount of study [6].

*Corresponding Author:
reem.hikmat@uomustansiriyah.edu.iq

Beyond the 5G system, some fundamental concerns that need to be solved include a more significant system capacity, higher data rate [7,8], an enhanced quality of service (QoS), reduced latency, and a better level of security compared to the 5G system [9].

The capacity to manage massive data volumes and very high data rates per device is essential for wireless networks that support 6G technology. It would also follow the tendencies of past generations, including adopting new technology and services. The new offerings are A.I., 3D mapping, intelligent wearables, implants, driverless cars, sensing, and computing reality gadgets [10]. In certain circumstances, it is expected that the per-user data rate in 6G will be close to one terabit per second [1,11]. It will deliver a simultaneous wireless connection one thousand times greater than the 5G system.

Metals, particularly gold, are the material of choice for constructing antennas that operate in the THz frequency regime. The poor conductivity of metal at the THz frequencies band, compared to its conductivity at D.C. frequencies, allows for increased field penetration into metal [12]. So, to reduce the losses in metallic antennas, it is proposed to investigate the use of nonmetallic materials. Graphene is the material of choice to get minimum losses in the THz region and is a brand-new substance made up of a single atom of graphite, a kind of carbon with a variety of exceptional electrical and mechanical properties [13]. It is considered the strongest and thinnest known material sheet. Its conductivity can be changed to behave like a semiconductor or a metal, which will make it an excellent choice for high-frequency electronics [14].

THz applications, such as imaging, spectroscopy, and others, have seen significant advancements in the last years [12]. Metals like gold are frequently used in the construction of antennas that operate at THz bands. Metallic antennas work at THz frequency scales and can penetrate more deeply and produce less radiation because the conductivity of metal is lower when measured at terahertz frequencies than it is at D.C. frequencies. [13]. To cut losses in smaller antennas, research into the use of nonmetallic materials is advised. The preferred material for reducing losses in the THz region is graphene. [14].

The need for a higher transmission capacity, a wider bandwidth, and Modern wireless communication methods have become more prevalent, which has led to better use of the available frequency range. The technically advanced advancement is utilizing many antenna components at both ends of the network. These wireless systems are called MIMO, meaning multiple inputs and outputs [15]. Without boosting transmit power or bandwidth, it offers a higher data rate [16]. It is a workaround for the data rate limitations imposed on single-input, single-output (SISO) systems. Additionally, MIMO may be implemented in different networks to improve the system's dependability, the speed at which data is sent, and the channel's performance [3,17]. In a MIMO antenna, the decreased distance between the antennas will increase the mutual coupling, resulting in more correlation coefficients and reduced efficiency and gain [18].

This paper presents a wideband, effective, and reconfigurable MIMO antenna based on graphene for THz applications.

2. Method

2.1. Conductivity of Graphene

Graphene is a substance that consists of only two dimensions and has a thickness of one atomic [18]. The graphene surface conductivity may be

broken down into two distinct categories: the first category, known as the intra-band, is Predominant in the below five THz, while the second category, known as the inter-band, predominates in the higher frequency ranges. Their effects on the surface conductivity of graphene can be seen on both sides of the equation [19].

$$\sigma = \sigma_{inter} + \sigma_{intra} \quad (1)$$

$$\sigma_{intra}(\omega, T, \mu_c, \gamma) = \frac{e^2 k_B T \tau}{\pi \hbar^2}\left[\frac{\mu c}{k_B T} + 2\ln\left(e^{\frac{-\mu_c}{k_{B.T.}}} + 1\right)\right]\frac{1}{\omega - j2\gamma} \quad (2)$$

$$\sigma_{inter}(\omega, T, \mu_c, \gamma) = \frac{-je^2}{4\pi\hbar}\ln\left(\frac{2|\mu_c| - (\omega - j2\gamma)\hbar}{2|\mu_c| + (\omega - j2\gamma)\hbar}\right) \quad (3)$$

μ_c is the Chemical potential in ev.

ω is the Angular frequency in rad/sec.

e is the Electron charge.

T is the temperature (Kelvin).

γ is the scattering rate (s^{-1}).

ħ is the reduced Planck's constant.

τ is the relaxation time.

Graphene's surface impedance may be calculated based on its conductivity using the equation provided below, where V_b is the applied voltage [20].

$$Z_S = {}^{1}/_{\sigma(\omega)} = R_S(V_b) + j\,X_S(V_b) \quad (4)$$

2.2. The Designed Single Antenna

Fig.1(a),(c) shows the proposed semi-hexagonal graphene microstrip patch antenna connected to a feed line with a width of Wf=3 µm, and its length Lf=8 µm that is designed by the microstrip equation in [21]. Two triangular-shaped slots have been carved into the radiating element's lower edge. A middle quadrilateral slot with a partial ground plane obtained Lg is equal to the quarter of the wavelength, and Wg is optimized as in Fig. 1(b),

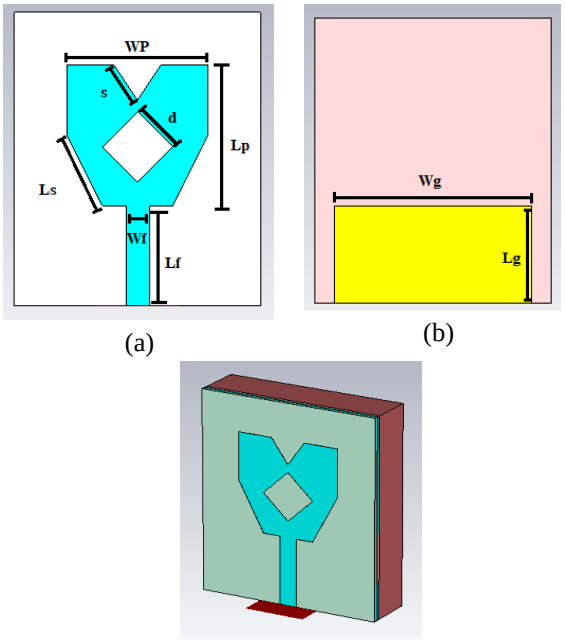

(a) (b)

(c)

Figure 1. The single design (a) front, (b) back, and(c) side view.

On the silicon dioxide (Sio2) dielectric substrate's front surface 40 x 45 μm^2 with ε_r=3.9 , The height is 10 μm, and two sub-layers above the silicon dioxide are the Alumina and silicon crystalline, each one has a thickness 1 μm. The antenna is composed of graphene elements with a relaxation time of 0.1 ps and a thickness of 0.001 nm. Table 1 shows the optimal dimensions of the designed antenna.

Table 1. The measurements of a single design

variables	Value (µm)	variables	Value (µm)
Wp	24	Wf	3
Lp	24	Lf	17
s	7.2	d	8.4
Ls	13.4	Wg	35
Lg	17	ds	28
ms	10		

The proposed antenna is developed and optimized by the full-wave electromagnetic computer modeling technique CST 2020. Fig.2

depicts the primary antenna setup, which works at the multi-band in the THz band and minimum return loss close to -50 dB. Fig.3 shows the radiation far-field, displaying a directivity of the main lob is 10.7dBi at f=9 THz. Fig.4 depicts the gain IEEE maximum value 11.06 dB at 9.5 THz.

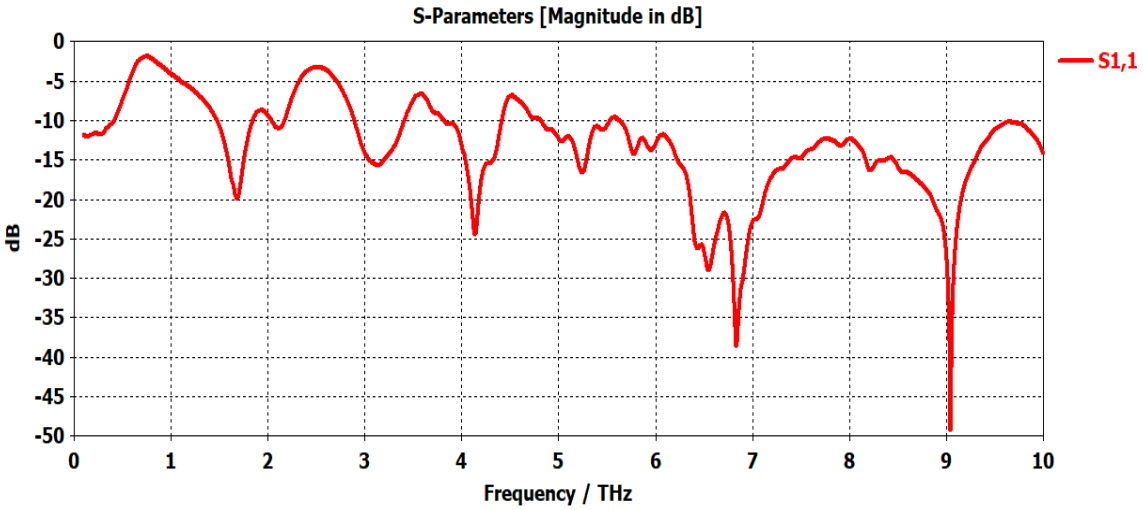

Figure 2. S_{11}

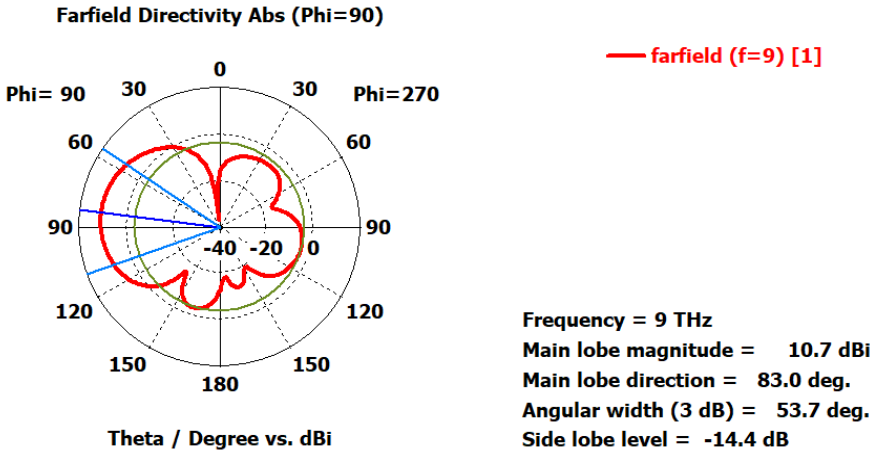

Figure 3. The far field radiation pattern at Frequency =9THz

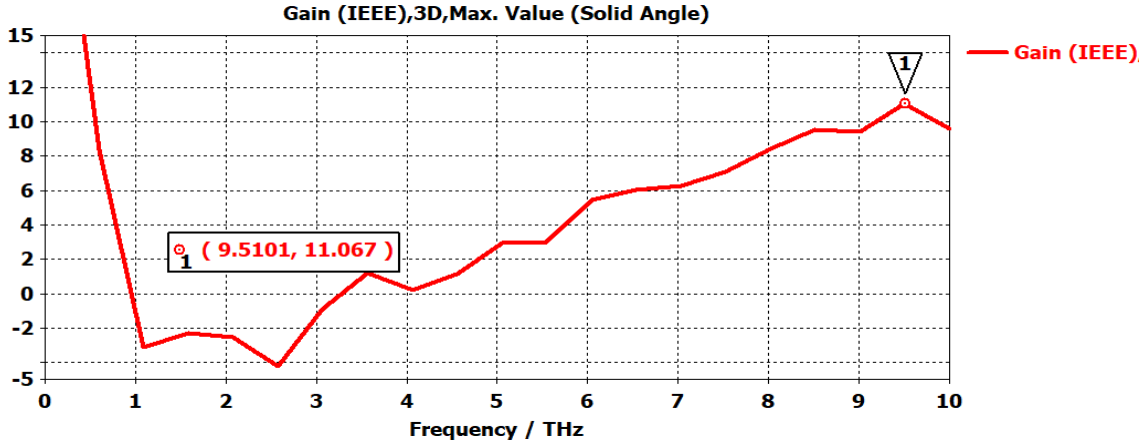

Figure 4. The single antenna gain IEEE

2.3 The design of the MIMO Antenna

A presented MIMO antenna is modified from the design's single antenna. It is then orthogonally arranged and placed on a substrate of silicon dioxide (SiO2) with a ten μm thickness, as shown in Fig. 5(a), (c). The MIMO antenna has overall dimensions of 90×90 μm^2. The ground is made of copperas represented in Fig.5(b). By making all of the ports orthogonal, each radiator's bottom borders are linked to the microstrip feed line to improve the isolation.

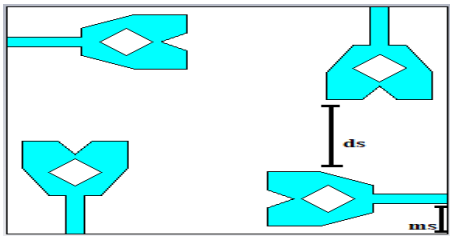

(a)

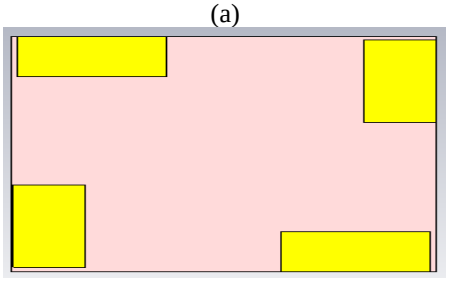

(b)

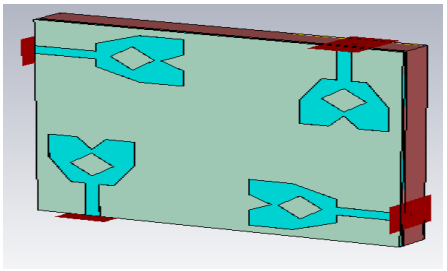

(c)

Figure 5. MIMO design (a) front, (b) back, (c) side view

The distance between each antenna is set at 28 µm according to ($\lambda/2$), as represented in Table 1, to lessen the co-reflection coefficient and boost the performance.

3. The Results

3.1. S-Parameters

The designed MIMO antenna works in multi-band with different values of µc that present a reconfigurable MIMO antenna that covers all the frequency bands (0.1-10) THz with mutual coupling -20 dB and less. The proposed MIMO antenna simulation results are obtained for various chemical potential values using Studio version 2020 CST. Fig. 6(a) represents the scattering parameter s_{11} and the mutual coupling in decibels for the suggested MIMO antenna's case Fig. 6(b) represents the reflection coefficient of all ports in the MIMO antenna at µc =1ev

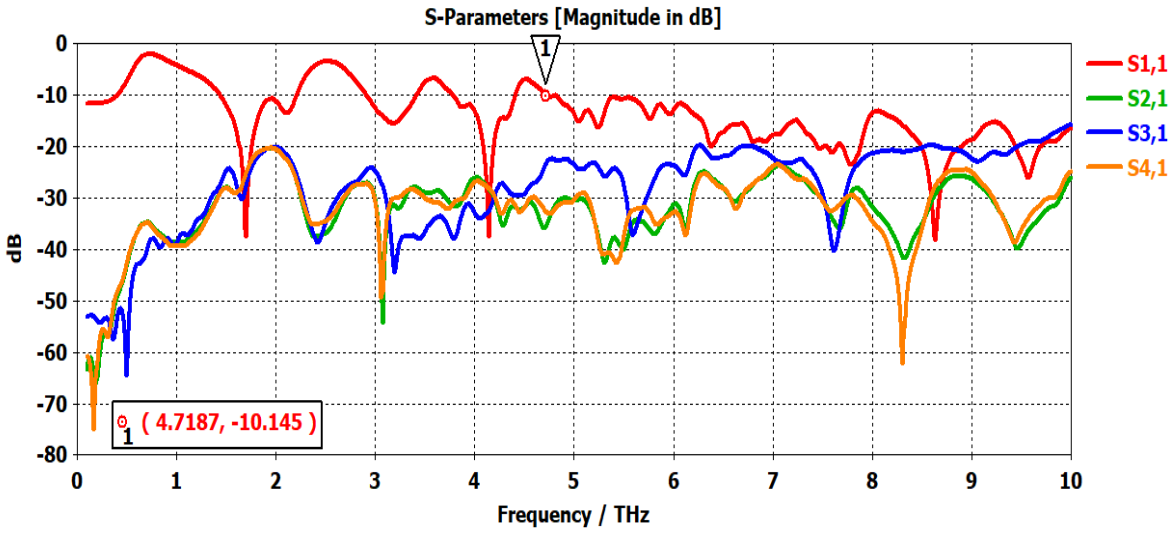

(a)

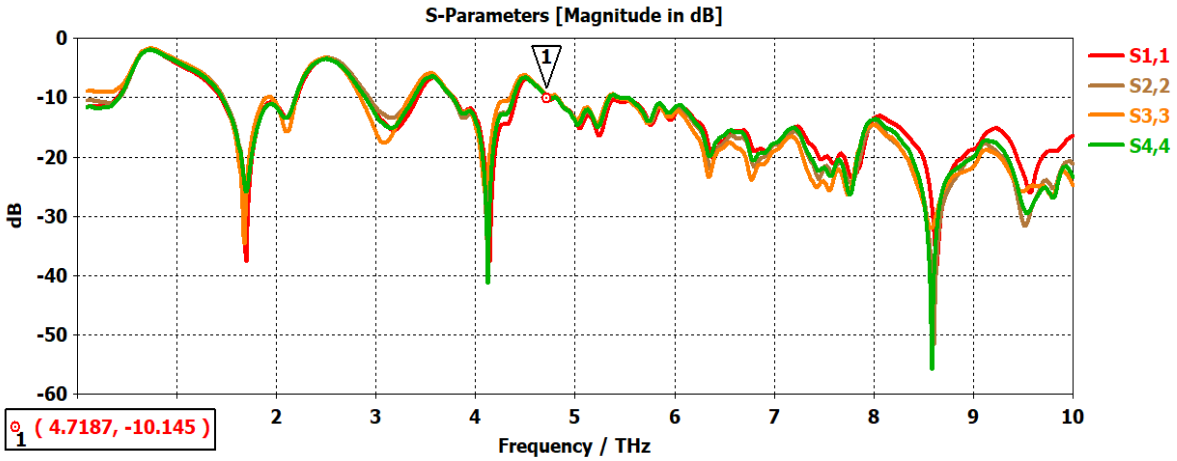

(b)

Figure 6. (a)The s_{11} and mutual coupling of antenna performance at µc =1ev (b) The reflection coefficient of the MIMO antenna at µc =1ev

The chemical potential will also shift whenever we adjust the D.C. voltage, but the return loss remains lower than -10 dB. The chemical potential changed the MIMO antenna bandwidth in Fig. 7,8,9, and 10. Because the antenna's chemical potential may be changed in response to the D.C. voltage that is delivered, it is possible to tune the antenna to a particular frequency.

This indicates that the return loss S_{11} at specific frequencies is less than -10dB, but at other frequencies, it is not. The return loss S_{11} at µc (0.1,0.3,0.5,0.7,1) shown in Fig. 11 shows that this MIMO antenna works for the entire (0.1-10) THz frequency band, so a reconfigurable MIMO antenna result.

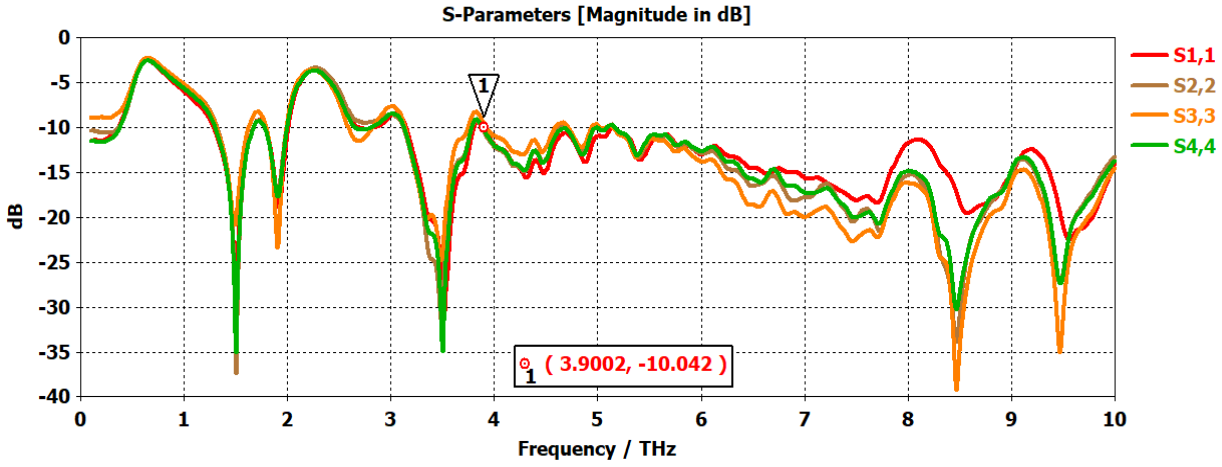

Figure 7. The MIMO antenna performance µc =0.7 ev

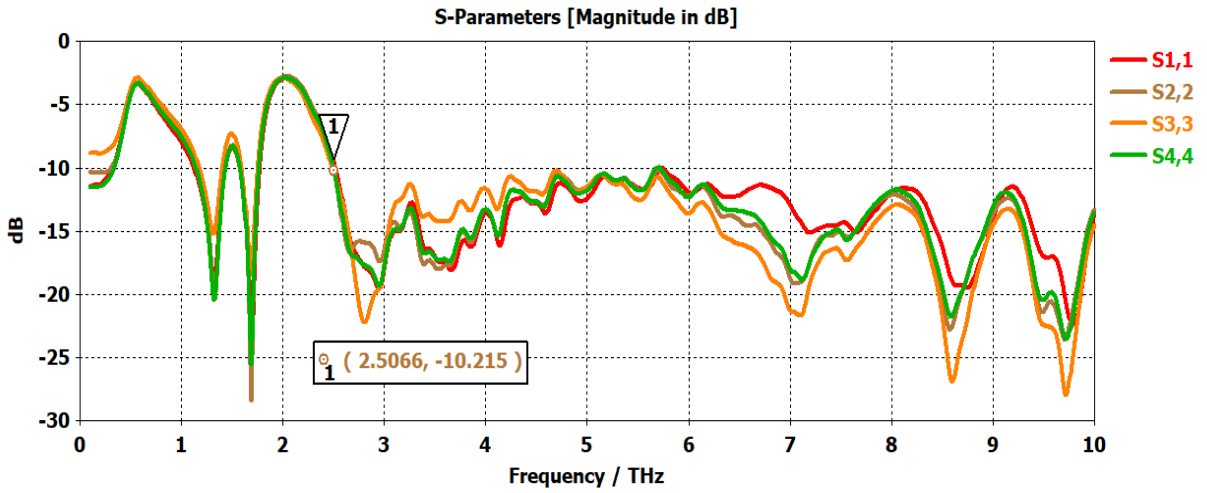

Figure 8. The MIMO antenna performance µc=0.5ev

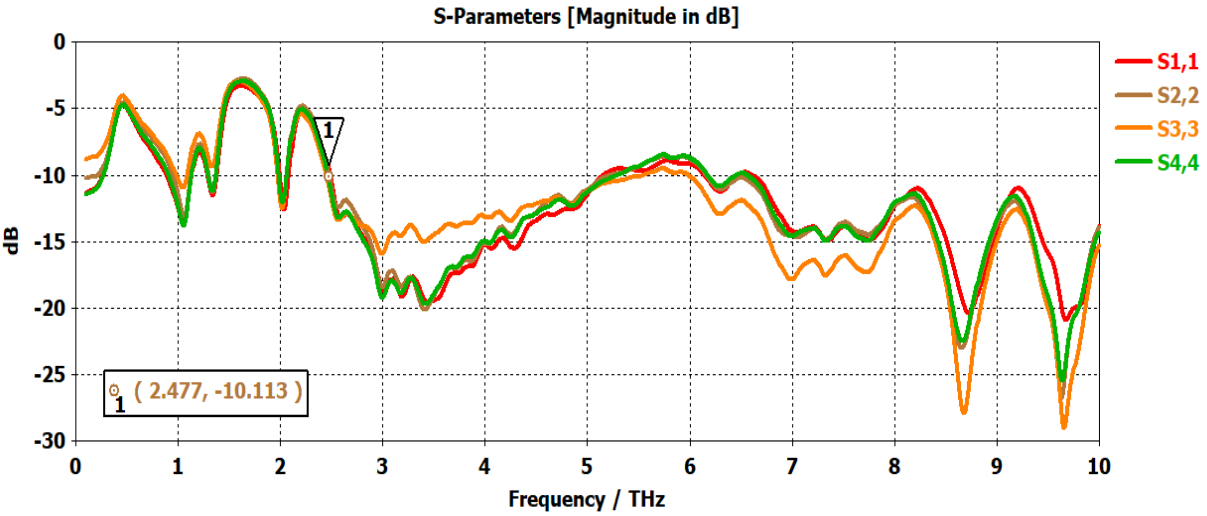

Figure 9. The MIMO antenna performance µc=0.3ev

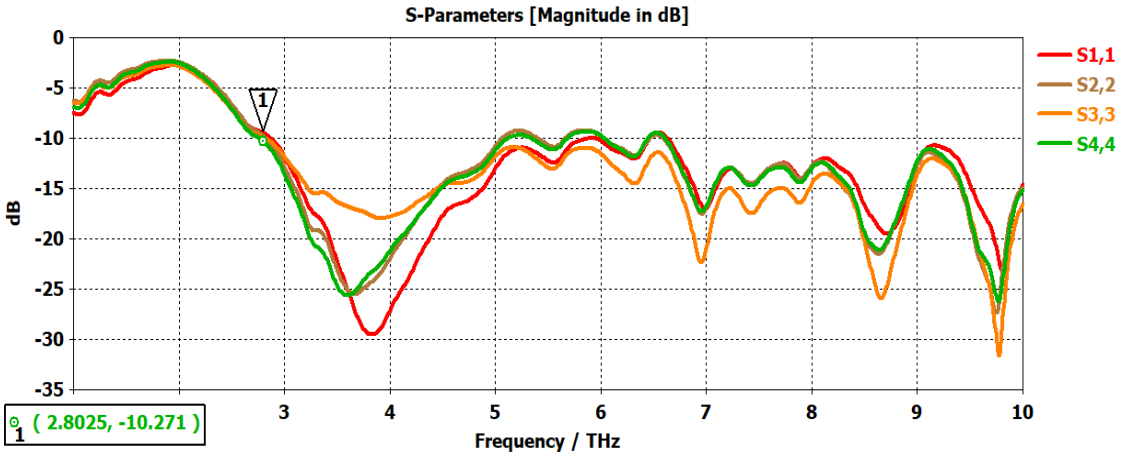

Figure 10. The MIMO antenna performance µc =0.1ev

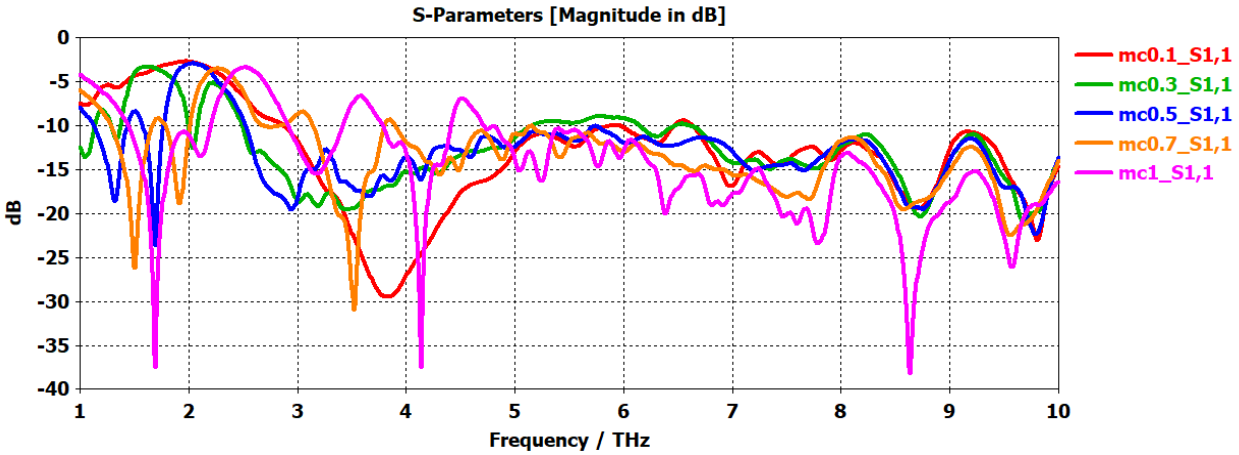

Figure 11. S_{11} of the MIMO antenna at μc = (0.1,0.3,0.5,0.7,1)ev

3.2. The far-field radiation pattern

The planned MIMO antenna far-field is depicted in Fig. 12 and 13, which show the realized gain that rises as the frequency of the band of interest increases.

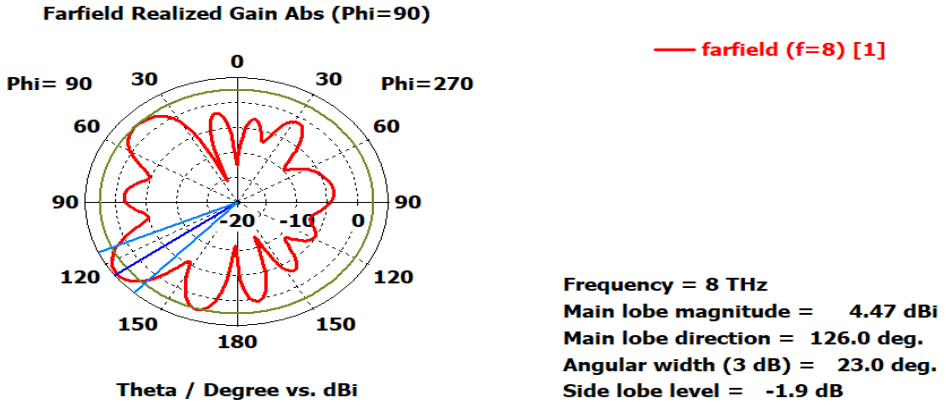

Figure 12. The far-field in 8 THz

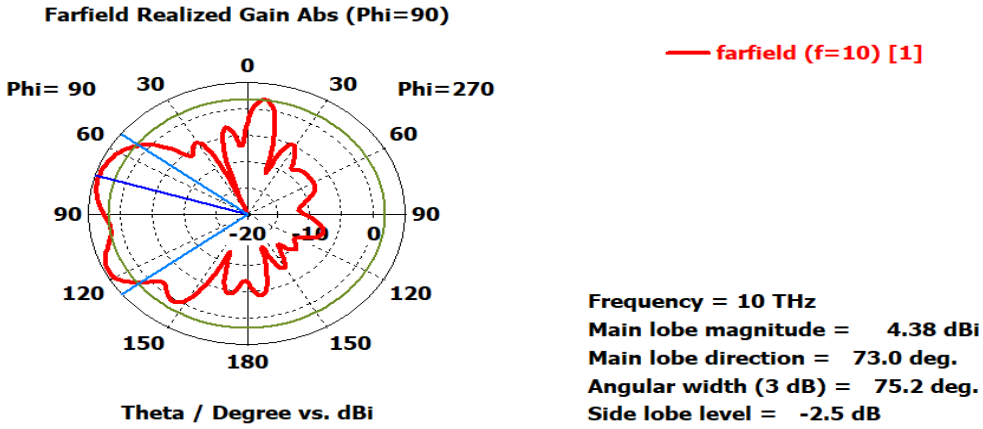

Figure 13. The far-field in 10 THz

3.3. The Gain, (ECC)Envelop Correlation Confliction and (DG) Diversity Gain:

A higher data rate for long-distance transmission is needed for the development of the MIMO design, which ensures the graphene antenna's compliance in the THz frequency band.

Fig.14 depicts the simulation of gain vs frequency for the present graphene-based MIMO antenna, demonstrating that the gain IEEE is above zero dB for all (0.1-10)THz since the graphene MIMO antenna works in THz band, with the peak gain value being 8.1dBi at 9.2 THz.

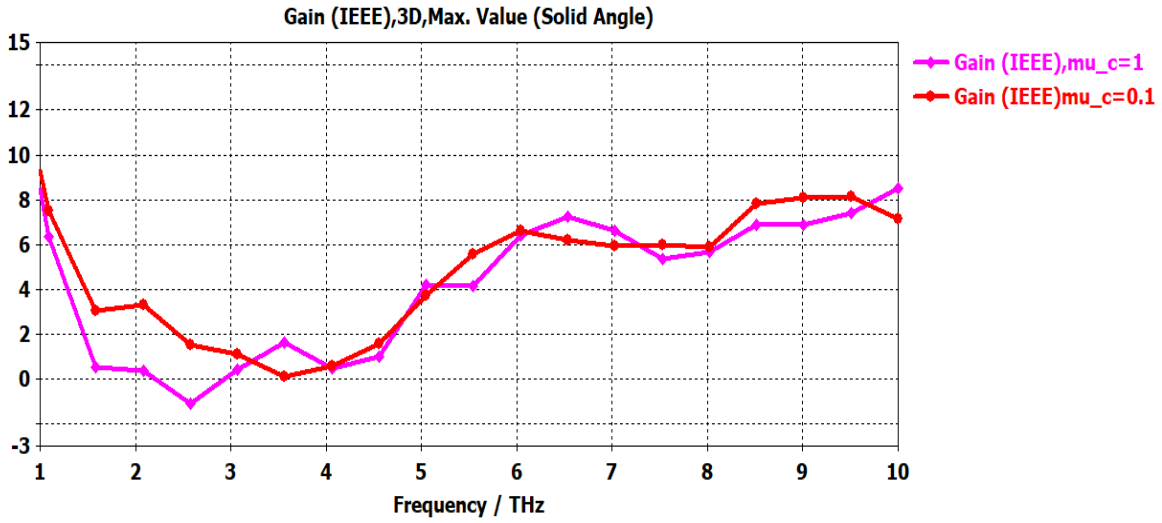

Figure 14. The gain IEEE of the MIMO antenna µc =0.1ev and µc =1ev

When attempting to determine whether or not the ports correlate with one another, the envelope correlation coefficient (ECC) must demonstrate that each channel is independent. It is less than 0.003 for all the THz bands, as shown in Fig. 15. The ECC value should be relatively small. And fall between 0 and 0.5. MIMO antennas must have very low ECC, which could be computed by using the S-parameters using the equation that shown below [22].

$$|\rho_{(ij)}|^2 = \rho_{(eij)} = \left| \frac{|S_{ii}^* S_{ij} + S_{ji}^* S_{jj}|}{\left|\left(1-|S|_{ii}|^2-|S|_{ji}|^2\right)\left(1-|S_{jj}|^2-|S_{ij}|^2\right)\eta_{radi}\,\eta_{radj}\right|^{(1/2)}} \right|^2 \quad (5)$$

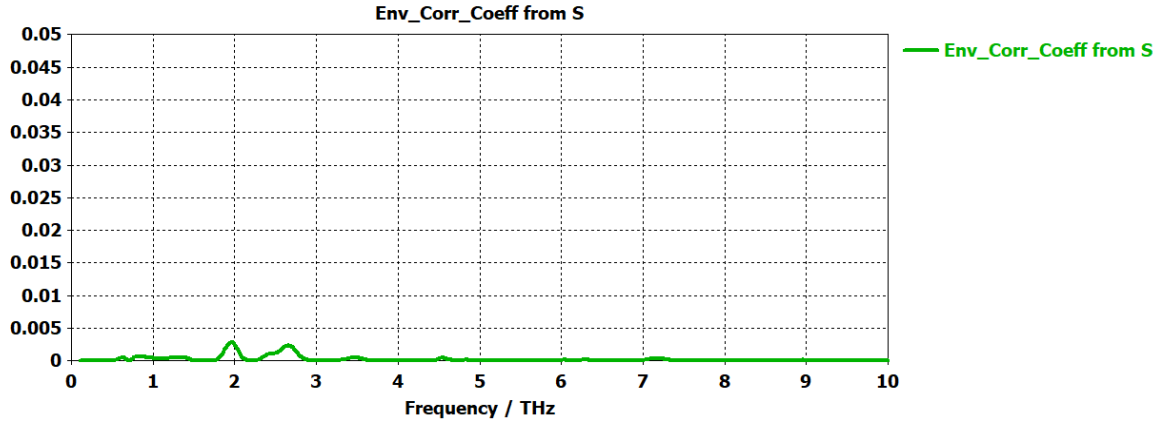

Figure 15. The Envelop correlation confliction (ECC)

The equation used to calculate the diversity gain of the proposed MIMO antenna is as follows [22](6):

$$DG = 10\sqrt{1-(ECC)^2} \quad (6)$$

To get a diversity benefit close to 10 dB, the correlation across ports should ideally be lower than 0.5. The outcomes of modeling diversity gain among radiating element ports are illustrated in Fig.16.

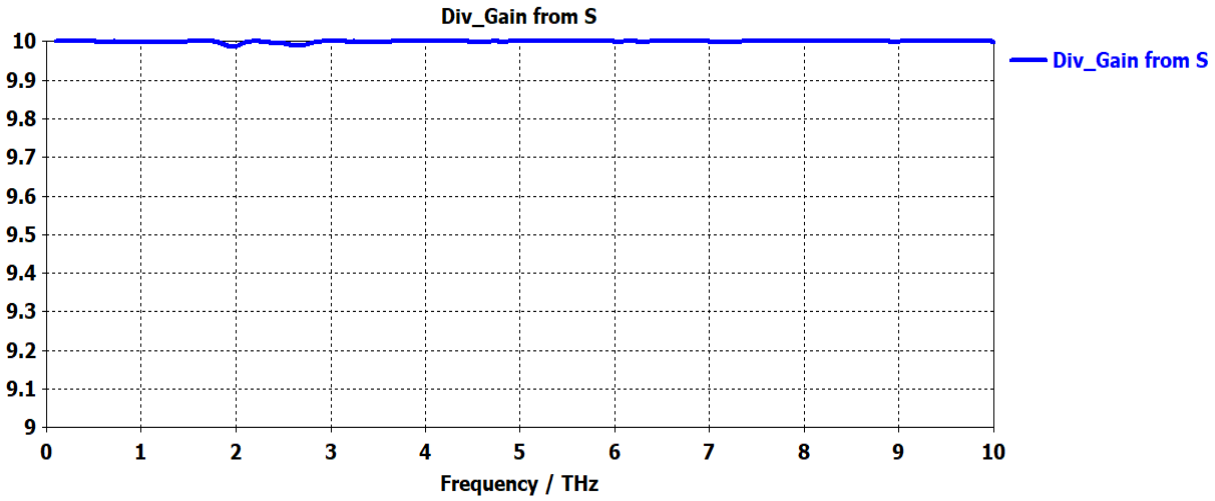

Figure 16. The DG for the MIMO antenna

The calculated value of the diversity gain of the graphene MIMO antenna is less than 9.99 over the whole spectrum, demonstrating that the suggested antenna has a suitable performance.

4. Conclusions

The design and numerical analysis of a reconfigurable four-element MIMO antenna intended for use in THz applications have been completed. In great depth, this study describes the development, design, and geometry of a valuable antenna for THz applications. The graphene MIMO antenna has a minimum return loss of around -50 dB and operates in a multi-band of THz band with different values of µc. The suggested MIMO antenna demonstrates a peak gain 8.4 dB in 10 THz, and its ECC is closer to 0.003 dB for each two ports of the MIMO antenna. This study concludes that raising the voltage applied to graphene strips reduces graphene surface impedances, resulting in the resonance frequency shifting towards higher frequencies. Therefore, the suggested MIMO antenna is appropriate for various THz applications due to its high gain, excellent diversity performance and steady radiation pattern examples of these applications include the diagnosis of breast cancer, the measurement of sugar, and the detection of drugs.

Acknowledgements

The authors acknowledge Mustansiriyah University for its support to improve the research quality

Conflict of interest

The authors guarantee that publishing this work will not result in any conflicts of interest for themselves or any other parties.

Author Contribution Statement

The author, Reem Hikmat, proposed the research problem and Dr Hussien A. Abdunabi supervised the results of this work. All authors contributed to writing and editing this manuscript. The authors, Dr Hussien A. Abdunabi and Reem Hikmat developed the introduction and style of the manuscript. All authors discussed the results and contributed to the final manuscript.

References

1. Devapriya, A.T., and Robinson, S,(2019). *Investigation on metamaterial antenna for terahertz applications*, Journal of Microwaves, Optoelectronics and Electromagnetic Applications, Vol. 18, issue 3, p-p 377-389, DOI: https://doi.org/10.1590/2179-10742019v18i31577.
2. Alharbi, A.G., and Sorathiya, V,(2022). *Ultra-Wideband Graphene-Based Micro-Sized Circular Patch-Shaped Yagi-like MIMO Antenna for Terahertz Wireless Communication*, Electronics, vol 11, Issue. 9, p-p 1305, DOI: https://doi.org/10.3390/electronics11091305.
3. Chowdhury, M. Z., Shahjalal, M., Ahmed, S., & Jang, Y. M.,(2020). *6G Wireless Communication Systems: Applications, Requirements, Technologies, Challenges, and Research Directions*. IEEE Open Journal of the Communications Society, vol. 1,p-p. 957 – 975, DOI: https://doi.org/10.1109/ojcoms.2020.3010270.
4. Akyildiz, I.F., Jornet, J.M., and Han, C., (2014). *Terahertz band: Next frontier for wireless communications*, Physical Communication, vol.12, p-p. 16-32, https://doi.org/10.1016/j.phycom.2014.01.006.
5. Tekbıyık, K., Ekti, A.R., Kurt, G.K., and Görçin, A., (2019).*Terahertz band communication systems: Challenges, novelties and standardization efforts*, Physical Communication, vol.35, p-p.100700, DOI: https://doi.org/10.1016/j.phycom.2019.04.014.
6. Mahdi, R.H., Abdulnabi, H.A., and Alsudani, A., (2022). *Plasmonic high gain graphene-based antenna array design for ultra-wideband terahertz applications*, Bulletin of Electrical Engineering and Informatics, vol. 11, Issue. 6, p-p 3322-3328, DOI: https://doi.org/10.11591/eei.v11i6.3673.
7. Koenig, S., Lopez-Diaz, D., Antes, J., Boes, F., Henneberger, R., Leuther, A., Tessmann, A., Schmogrow, R., Hillerkuss, D., and Palmer, R. (2014). Wireless sub-THz communication system with high data rate enabled by R.F. photonics and active MMIC technology. in 2014 IEEE Photonics Conference, DOI: https://doi.org/10.1109/ipcon.2014.6995424
8. Poorgholam-Khanjari, S., and Zarrabi, F.B., (2021). *Reconfigurable Vivaldi THz antenna based on graphene load as hyperbolic metamaterial for skin cancer spectroscopy*, Optics Communications, vol. 480, p-p. 126482, DOI: https://doi.org/10.1016/j.optcom.2020.126482.
9. Rasheed, F.M., and Abdulnabi, H.A (2022). Multiband graphene-based Mimo antenna in terahertz antenna regime, 2022 2nd International Conference on Computing and

Machine Intelligence (ICMI), DOI: https://doi.org/10.1109/icmi55296.2022.9873789.

10. Geetharamani, G., and Aathmanesan, T., (2020). *Split ring resonator inspired THz antenna for breast cancer detection*, Optics & Laser Technology, vol.126, p-p. 106-111, DOI:https://doi.org/10.1016/j.optlastec.2020.106111.

11. Abdualnabi, H. A., Al-Aboosi, Y. Y., and Sallomi, A. H., (2020). Photonic Antenna Design for Long Term Evolution Application, in IOP Conference Series: Materials Science and Engineering. DOI: https://doi.org/10.1088/1757-899x/881/1/012147.

12. Saad, W., Bennis, M., and Chen, M,(2020). *A Vision of 6G Wireless Systems: Applications, Trends, Technologies, and Open Research Problems*, IEEE Network, vol. 34, Issue. 3, p-p 134- 142, DOI: https://doi.org/10.1109/mnet.001.1900287.

13. Hanson, G. W. (2008). *Radiation Efficiency of Nano-Radius Dipole Antennas in the Microwave and Far-infrared Regimes*, IEEE Antennas, vol. 50, Issue. 3, p-p 66–77, DOI: https://doi.org/10.1109/map.2008.4563565.

14. David, K., and Berndt, H, (2018). *6G Vision and Requirements: Is There Any Need for Beyond 5G?* IEEE Vehicular Technology Magazine, vol. 13, Issue. 3, p-p 72 - 80, DOI: https://doi.org/10.1109/mvt.2018.2848498.

15. Rasheed.F.M, and Abdulnabi.H.A (2022). *Toothed log periodic graphene-based antenna design for THz applications*, Bulletin of Electrical Engineering and Informatics, vol. 11, no. 6, p-p 3346- 3352, DOI: https://doi.org/10.11591/eei.v11i6.4256.

16. Khan, M.I., Khan, S., Kiani, S.H., Ojaroudi Parchin, N., Mahmood, K., Rafique, U., and Qadir, M.M., (2022*), A Compact mmWave MIMO Antenna for Future Wireless Net.works*, Electronics, vol. 11, Issue. 15, p-p 2450, DOI: https://doi.org/10.3390/electronics11152450.

17. Song, R., Chen, X., Jiang, S., Hu, Z., Liu, T., Calatayud, D.G., Mao, B., and He, D. A,(2021). *A Graphene-Assembled Film Based MIMO Antenna Array with High Isolation for 5G Wireless Communication*, Applied Sciences, vol. 11, Issue. 5, p-p 2382, DOI: https://doi.org/10.3390/app11052382.

18. Varshney, G., Gotra, S., Pandey, V., and Yaduvanshi, R.S.,(2019), *Proximity-coupled two-port multi-input-multi-output graphene antenna with pattern diversity for THz applications*, Nano Communication Networks, vol. 21, p-p 100246, DOI: https://doi.org/10.1016/j.nancom.2019.05.003.

19. Dwivedi, A.K., Sharma, A., Singh, A.K., and Singh, V. (2020), *Circularly Polarized Two Port MIMO Cylindrical DRA for 5G Applications. in 2020* International Conference on UK-China Emerging Technologies (UCET), DOI: https://doi.org/10.1109/ucet51115.2020.9205408.

20. Abdulnabi, H.A., Hussein, R.T., and Fyath, R.S., (2017). *UWB Single Port Log Periodic Toothed Terahertz Antenna Design Based on Graphene Artificial Magnetic Conductor*, Modern Applied Science, vol.11, Issue. 3, p-

p 86, DOI: https://doi.org/10.5539/mas.v11n3p86.

21. Bhalla, D. and K. Bansal, (2013), *design of a rectangular microstrip patch antenna using inset feed technique*, IOSR Journal of Electronics and Communication Engineering, vol .7, Issue.4, p-p 08-13, DOI: https://doi.org/10.1109/apace53143.2021.9760620.

22. Achilles D. Boursianis, Sotirios K. Goudos, Traianos V. Yioultsis, Katherine Siakavara, and Paolo Rocca, (2020). *MIMO Antenna Design for 5G Communication Systems Using Salp Swarm Algorithm*, 2020 International Workshop on Antenna Technology (iWAT), DOI: https://doi.org/10.1109/iwat48004.2020.1570618331.